ISSN 1061-9348, Journal of Analytical Chemistry, 2015, Vol. 70, No. 10, pp. 1254–1260. © Pleiades Publishing, Ltd., 2015.

ARTICLES

The Electrochemical Study of Glucose Oxidase on Gold-Coated Magnetic Iron Oxide Nanoparticles[1]

Khadijeh Eskandari[a], Hajar Zarei[b, c], Hedayatollah Ghourchian[d,*], and Seyed-Mostafa Amoozadeh[a]

[a] *Nanobiotechnology Research Center, Baqiyatallah University of Medical Science Tehran, Iran*

[b] *Department of Energy Engineering and Physics, Faculty of Physics, Amirkabir University of Technology Tehran, Iran*

[c] *Persian Gulf Research and Studies Center, Persian Gulf university Bushehr, Iran*

[d] *Laboratory of Microanalysis, Institute of Biochemistry and Biophysics, University of Tehran P.O. Box 13145-1384, Tehran, I.R. Iran*

**e-mail: hadi@ibb.ut.ac.ir*

Received February 11, 2014; in final form, January 31, 2015

Abstract—A feasible and fast method for glucose oxidase (**GOx**) study was developed by covalent attachment of GOx to gold-coated magnetic iron oxide nanoparticles (**Fe@Au**).GOx molecules were oxidized with metaperiodate to form aldehyde group. The prepared **Fe@Au** composite nanoparticles with 60 nm diameter were used as a carrier for the immobilization of GOx. Fe@Au nanoparticles were modified by cysteamine to produce amine groups at the surface. The GOx was covalently attached to the amine-modified Fe@Au nanoparticles through its aldehyde groups. The direct electrochemistry of GOx showed a quasi-reversible cyclic voltammogram corresponding to the flavin adenine dinucleotide (**FAD/FADH$_2$**) redox couple with a formal potential of –270 mV in 0.1 M phosphate buffer. The apparent charge transfer rate constant (k_s) and transfer coefficient for electron transfer between the electrode surface and enzyme were calculated as 2.23 s^{-1} and 0.45, respectively. The linear concentration range of the biosensor is 2.4–54 mM with detection limit of 0.51 mM at $S/N = 3$. The apparent Michaelis–Menten constant was measured to be 8.59 mM, indicating that the immobilized GOx on Fe@Au preserved its native activity. The life time of biosensor is more than 2 weeks.

Keywords: biosensor, direct electrochemistry, glucose oxidase, gold-coated iron oxide nanoparticles, immobilization

DOI: 10.1134/S1061934815100123

The determination of glucose concentration is very important in clinical, biological and chemical samples, as well as food processing and fermentation [1]. Chiefly glucose sensors have been studied most extensively because of their need in diagnostic analysis of diabetes [2]. In the last few years, considerable attention has been devoted to immobilization of enzymes on electrode surface in relation to the development of electrochemical biosensors [3] that are popular because of high sensitivity, simple and low-cost instrumentation and easy signal amplification [4]. Due to active usage of glucose biosensor and economic prospects, it has led to a considerable amount of fascinating research and innovative detection strategies that could improve the simplicity, sensitivity, stability and selectivity [5]. Electrode surface modification with metal nanoparticles is one of the best strategies for improving glucose biosensor in place of conventional sensing technologies, which has led to improve sensitivity, selectivity, and stability of assay.

Metal nanoparticles are of considerable interest as they exhibit unique electronic, optical, and catalytic properties due to the quantum size effects [6]. However, the gold nanoparticles are expected to exhibit attractive properties in the application to glucose biosensors because of their highly conducting material, high surface, good biocompatibility and simple synthetic procedure [7].

On the other hand, nowadays the magnetic nanoparticles receive increasing attention in designing electrochemical enzyme biosensors [8, 9]. Magnetic nanoparticles as the immobilization platforms have some advantages such as: (1) few fouling, selective and fast separation of the immobilized enzymes from the reaction mixture by the application of a magnetic field; (2) enzyme immobilization over the higher specific surface area to bind a large amount of enzymes; (3) low mass transfer resistance; (4) immobilization of enzyme on electrode without the need for any chemical linker or electrode modification by magnetic force; (5) simple regeneration of magnetic-modified electrodes by removing the magnetic field [10–12]. Fe@Au nanoparticles in comparison to other magnetic nanoparticles are more common due to simplicity of synthesis, inherent biocompatibility, powerful

[1] The article is published in the original.

super-paramagnetic effects, low toxicity and cost [13]. Fe@Au nanoparticles area very attractive composite system with synergetic properties that leads to the improvement in the biosensor performance. Fe@Au nanoparticles exhibit interesting electrochemical and biocompatible properties due to Au and magnetic properties of Fe_3O_4. However, to the best of our knowledge, up to now there is no report on applying Fe@Au nanocomposite as an immobilizing platform for developing electrochemical glucose biosensor.

In this work, covalent immobilization of GOx on amine-modified Fe@Au nano-compositeis introduced as a new platform for constructing glucose electrochemical biosensor using cyclic voltammetery (**CV**) and square wave voltammetery (**SWV**) modes.

EXPERIMENTAL

Materials. GOx (EC 1.1.3.4, Type X-S from *Aspergillus niger*) and β-D-(+)-glucose were purchased from Sigma and used as received. $FeCl_2 \cdot 7H_2O$, $FeCl_3 \cdot 6H_2O$, NaOH, HCl, tetramethyl ammonium hydroxide (**TMAOH**) pentahydrate were purchased from Sigma-Aldrich (Steinheim, Germany). Chloroauric acid trihydrate ($HAuCl_4 \cdot 3H_2O$), potassium trisodium citrate, sodium metaperiodate, ethylene glycol, potassium dihydrogen phosphate (KH_2PO_4) and potassium hydrogen phosphate (K_2HPO_4) were purchased from Merck and used as delivered. The solutions were prepared in deionized double distilled water (18 MΩ cm, Barnstead, Dubuque, USA) and all experiments were carried out at room temperature (25°C).

Apparatus and measurements. All electrochemical experiments were performed with an Autolab potentiostat (PGSTAT 101). Electrochemical studies were performed using a single-compartment conventional three-electrode cell (volume 300 μL). A gold-disk working electrode with a diameter of 2 mm equipped with a permanent magnet under it, a saturated silver/silver chloride (Ag/AgCl) reference electrode, containing 3 M KCl (from Azar electrode, Iran), and a platinum rod auxiliary electrode were used. All potentials were measured and reported versus the Ag/AgCl reference electrode. The morphology of the synthesized Fe@Au nanoparticles was obtained using a scanning electron microscope (**SEM**) Model LEO 440i, UK. The UV-Vis spectra were carried out using a Cary spectrophotometer, 100 Bio-model (Japan). The electrochemical behavior of GOx and detection of glucose was carried out in an air-saturated solution for similarity of in vivo usage.

Preparation of the gold-coated iron oxide nanoparticle (Fe@Au). The Fe@Au was prepared by the procedures described in literature [14]. In short, 5.4 g $FeCl_2 \cdot 7H_2O$ and 2.0 g $FeCl_3 \cdot 6H_2O$ were dissolved in 25 mL of 10 mM HCl and the solution was added drop wise to 250 mL of 1.5 M NaOH solution under vigorous stirring. A black precipitate was immediately formed. It was washed with distilled water to remove the NaOH excess and heated at 60°C to dryness. In order to encapsulate the iron nanoparticles with the gold shells, 5 mL of iron oxide nanoparticles suspended in 0.1 M TMAOH solution (pH12) was added to 95 mL of citric acid (5 mM) and stirred vigorously. Finally, 0.2 M $NH_2OH \cdot HCl$ and 1% $HAuCl_4 \cdot 3H_2O$ were alternatively added into the magnetite solution until the solution became purple.

Oxidation of glucose oxidase. GOx molecule was oxidized with periodate to convert carbohydrate–OH groups on the peripheral surface of the protein to aldehydes according to established procedures [15]. Briefly, 1 mL of 10 mg/mL GOx solution provided in 0.1 M phosphate buffer solution (**PBS**, pH 6.8) was reacted with 30 mg of sodium metaperiodate for 15 min at room temperature in the dark. The reaction was stopped with the addition of 10 μL of ethylene glycol (30 min, 25°C). Finally, the oxidized GOx was dialyzed (molecular weight cutoff 30000) against PBS (pH 6.8) for overnight at 4°C and freeze-dried.

Surface modification of the Fe@Au and electrode preparation. The modified gold-coated magnetic nanoparticles were prepared in two sequential steps: at the first step, 100 μL of 0.01 M cysteamine was added to 500 μL of suspended Fe@Au and the mixture was stirred for 20 min. The modified NH_2–Fe@Au nanoparticles were collected by magnet and the additional cysteamine was removed. At the second step, the activated NH_2–Fe@Au nanoparticles were equilibrated in phosphate buffer (0.1 M, pH 6.8), and transferred to the 20 μL (10 mg/mL) solution of oxidized GOx followed by shaking at 180 rpm for 5 h. During this step, the amine groups on NH_2–Fe@Au reacted with the aldehyde groups of the GOx, giving rise to covalent bonds. Then, to remove the additional and loosely bound GOx molecules, GOx/NH_2–Fe@Au were collected by a permanent magnet and washed with the PBS three times. GOx bearing NH_2–Fe@Au was fixed on the gold plate electrode using a permanent magnet. The prepared electrode was stored at 4°C before use.

RESULTS AND DISCUSSION

UV-Vis spectroscopic and SEM characterization of synthesized Fe@Au nanoparticles. The UV-Vis absorption spectra of iron oxide nanoparticles, Au nanoparticles as reference samples and Fe@Au nanoparticles were observed (Fig. 1). The black magnetic nanoparticle do not show absorption peaks in UV-Vis spectra (spectrum *1*). Red color gold colloid and Fe@Au colloid with a black-red color do exhibit an absorption band with maxima at 526 and 538 nm, respectively. The result show confirms the gold coating of the iron oxide nanoparticles in spectrum (spectrum *3*). Furthermore, spectrum (*3*) is broader than spectrum (*2*). The red shift and broadening in the surface plasmon

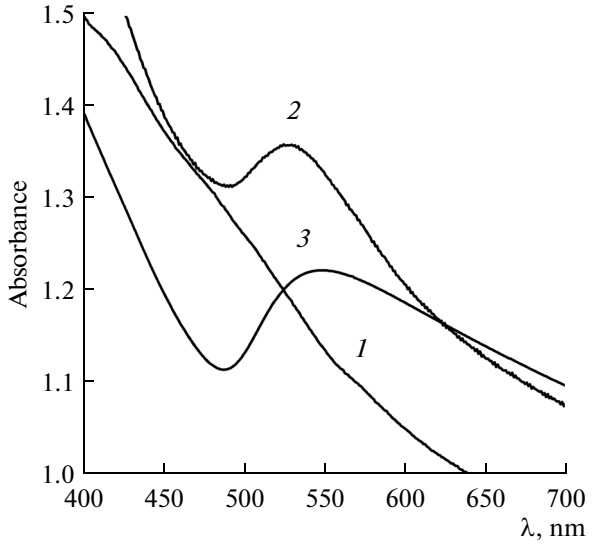

Fig. 1. UV-Vis absorption spectra of Fe_3O_4 nanoparticles (*1*), Au nanoparticles (*2*), Fe@Au nanoparticles (*3*).

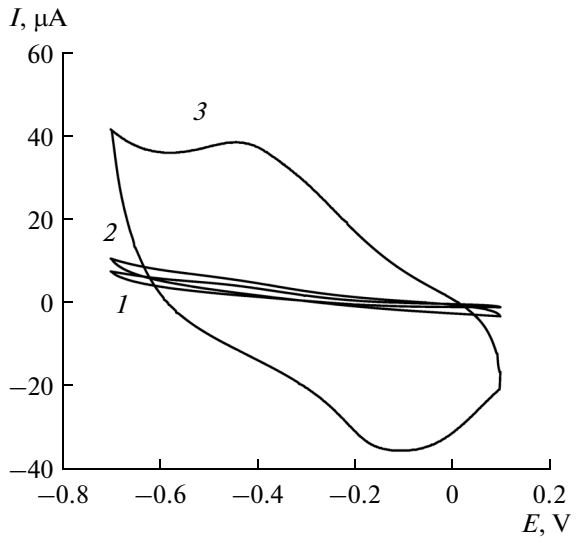

Fig. 3. CVs of bare gold electrode (*1*), Fe@Au/Au electrode (*2*), GOx/Fe@Au/Au electrode (*3*) in 0.1 M PBS (pH 6.8). The scan rate was 50 mV/s at air-saturated conditions.

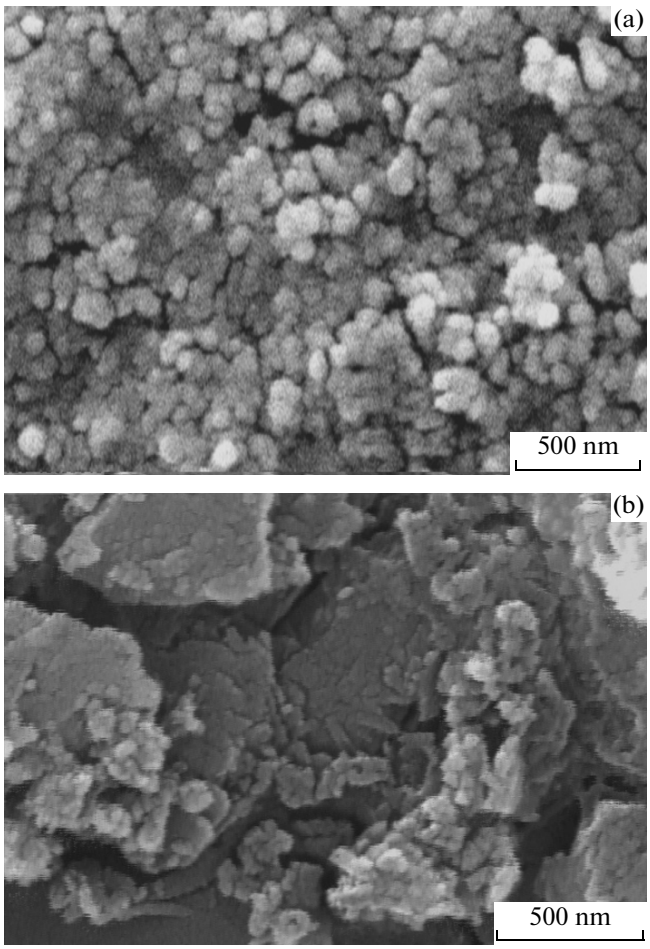

Fig. 2. SEM images of Fe@Au nanoparticles (a) and GOx/NH_2–Fe@Au (b) on Au electrode.

absorption of the Fe@Au colloid relative the pure Au colloid reveals that the size distribution of pure Au nanoparticles is narrower than that of the Fe@Au nanoparticles and the aggregation of Fe@Au nanoparticles is wider than the pure Au nanoparticles [11].

GOx bearing NH_2–Fe@Au were fixed on the gold plate electrode using a permanent magnet. Figure 2 shows the SEM images of Fe@Au (a) and GOx/NH_2–Fe@Au (b) after dropping on gold electrode and evaporating in air. Figure 2a shows the Fe@Au is spherical and their average diameter is around 50 nm. Also, it is clear in Fig. 2b that the morphology of Fe@Au was changed by addition of GOx. This indicates that the GOx has been successfully immobilized onto NH_2–Fe@Au surface.

Electrochemical properties of GOx on Fe@Au electrode. The direct electrochemistry of GOx immobilized on NH_2–Fe@Au/Au electrode was investigated using CV. Figure 3 shows the CVs of the bare Au electrode (*1*), NH_2–Fe@Au and GOx/NH_2–Fe@Au/Au electrode, (*2*) and (*3*), respectively, in 0.1 M PBS (pH 6.8) and air-saturated conditions. Neither curve (*1*) nor (*2*) shows redox peaks. However, it is obvious that the modified electrode exhibits excellent and quasi-reversible redox peaks, as shown in curve (*3*). At the same time, the NH_2–Fe@Au/Au electrode did not show any response. The anodic and cathodic peak potentials were –350 and –190 mV, respectively, with a peak potential separation of 160 mV. The direct electron transfer of GOx immobilized onto the heterogeneous surface is due to the redox reaction of FAD, which is bound to the enzyme molecule and can be expressed as [16]:

$$GOx{-}FAD + 2H + 2e \longrightarrow GOx{-}FADH_2. \quad (1)$$

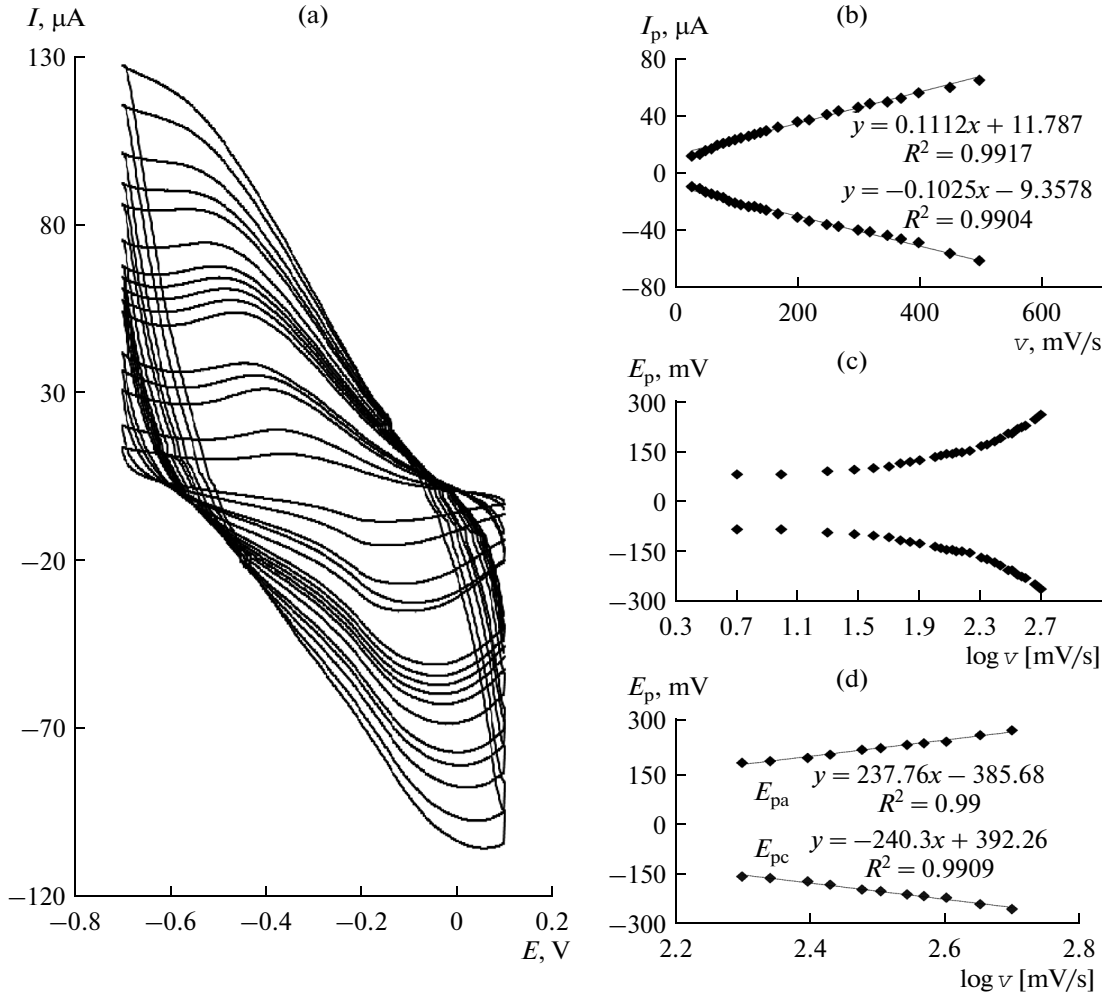

Fig. 4. CVs of GOx/Fe@Au/Au electrode in 0.1 M PBS (pH 6.8) at various scan rates of 5, 10, 20, 30, 50, 60, 70.80, 90, 100, 120, 150, 170, 200, 250 and 300 mV/s from inner to outer, respectively (a); plot of I_p vs. v (b); plot of E_p vs. log v (c); plot of E_{pa} and E_{pc} vs. log v (d).

The formal potential (E^0) has been calculated by average of the cathodic and anodic potentials that is −270 mV (vs. Ag/AgCl) for GOx. This result suggests that most of the GOx molecules preserved their native structure after the covalent attachment on magnetic nanoparticles.

Figure 4a shows the cyclic voltammograms of GOx/NH_2–Fe@Au/Au electrode in PBS (0.1 M, pH 6.8) at different scan rates. Figure 4b shows the plot of cathodic and anodic peaks current (I_p) against the scan rate (v). Both the anodic and cathodic peak currents increased linearly with square scan rate in the region of 5–500 mV/s indicating surface controlled redox reaction, as expected for immobilized systems [17].

The kinetic parameters of electron transfer coefficient (α) and apparent charge transfer rate constant (k_s) can be calculated using Laviron's model [18]. Laviron derived general expressions for the linear potential sweep voltammetric response for the case of surface-confined electroactive species at small concentrations, Eqs. (2)–(5):

$$E_{pc} = E^0 + \frac{RT}{(1-\alpha)nF}\ln\left[\frac{(1-\alpha)}{m}\right], \quad (2)$$

$$E_{pa} = E^0 + \frac{RT}{(1-\alpha)nF}\ln\left[\frac{\alpha}{m}\right], \quad (3)$$

$$E_{pa} - E_{pc} = \Delta E_p > \frac{200}{n}\text{mV}, \quad (4)$$

$$k_s = \alpha\log(1-\alpha) + (1-\alpha)\log\alpha - \log\left(\frac{RT}{nFv}\right) - \frac{\alpha(1-\alpha)nF\Delta E_p}{2.3RT}, \quad (5)$$

where $m = (RT/F)(k_s/n)$, k_s is the apparent charge transfer rate constant, v is the charge transfer coefficient, n is the number of electrons transferred in the

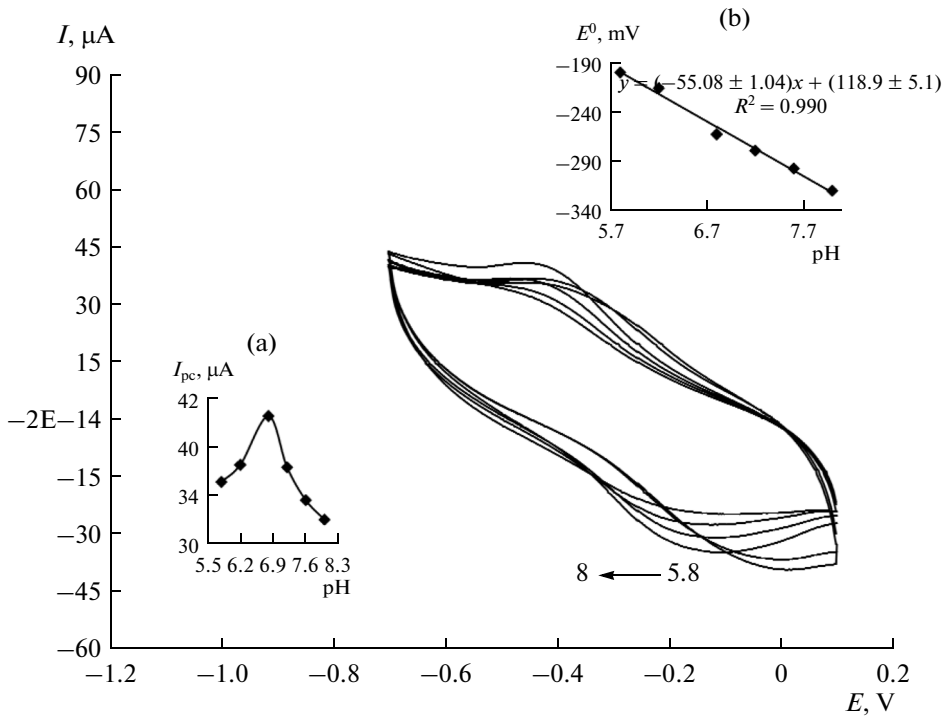

Fig. 5. CVs of GOx/Fe@Au/Au electrode in 0.1 M PBS at pH 5.8, 6.2, 6.8, 7.2, 7.6 and 8.0 from right to left, respectively. Insets (a) and (b) show the plot of I_{pc} vs. pH and E^0 vs. pH, respectively. The scan rate was 50 mV/s at air-saturated conditions.

rate-determining reaction, ΔE_p is the peak potential separation; R, T, and F have their usual meanings (R = 8.314 J/(mol K), T = 298 K, F = 96483 C/mol) and v is the scan rate. α can be calculated using the plot of peak potentials (E_p) vs. logarithm of scan rate (log v).

The slope of the linear section in cathodic and anodic peaks in Fig. 4c is equal to $-2.303RT/\alpha_c F$ and $2.303RT/\alpha_a nF$, respectively. As seen in Fig. 4d, it was found that for scan rates above 200 mV/s, $\Delta E = \Delta E_p - \Delta E^{0'}$ was proportional to the log v, as indicated by Laviron. Therefore, we extracted the average value of 0.25 and 1.4 s^{-1} for α and k_s, respectively. The obtained k_s value is higher than that reported for GOx immobilized on self-assembled monolayer (0.026 s^{-1}) [19] and close to GOx immobilized on CNTs (1.53 s^{-1}) [20].

Using Eq. (6), the amount of glucose oxidase (Γ) immobilized on the NH_2–Fe@Au/Au electrode was estimated to be 1.68×10^{-12} mol/cm.

$$I_p = \frac{n^2 F^2 v A \Gamma_c}{4RT}, \quad (6)$$

where v is the sweep rate, A is the surface area (0.0314 cm^2) of the modified electrode, and the other symbols are well-known constants. From the slope of cathodic peak currents vs. scan rate, the surface concentration of GOx is calculated. This suggests the formation of an approximate monolayer of GOx on the surface of the NH_2–Fe@Au/Au electrode. This value is close to those obtained at GOx/CdTe–CNTs/Nafion/GC electrode (8.77×10^{-11} mol/cm) [21] and GOx–SWNTs/GC electrode (2.85×10^{-13} mol/cm) [22].

Effect of pH on the peak potential. The voltammetric behavior of the GOx/NH_2–Fe@Au/Au electrode was investigated at various pH by CV. Figure 5 shows peak currents of the electrode in PBS at various pH ranging from 5.8 to 8. As seen in Fig. 5, the cathodic peak current rose with pH change from 5.8 to 6.8 and then decreased from pH 6.8 to 8. The maximum cathodic current was obtained at pH 6.8, therefore it was chosen as the optimal pH for further experiments.

As illustrated in Fig. 5 (inset b), the formal potential (E_0) of GOx/NH_2–Fe@Au/Au electrode would be linearly pH dependent. An increase in solution pH caused a negative shift in both cathodic and anodic peak potentials. The results showed that the slope (E^0/pH) is 55.08 mV/pH over a pH range from 5.8 to 8. This slope was close to the Nernstian value of 59.2 mV for a two-electron, two-proton process [16].

Determination of glucose by square wave voltammetry. As described above, direct electrochemistry of GOx occurs according to Eq. (1). In air saturated condition, oxidized GOx produced in Eq. (7) reacts with O_2 to reproduce reduced GOx (Eq. 8), oxygen is used as the electron acceptor. The electrocatalytic process is expressed as follows [23]:

$$GOx(FAD) + 2e + 2H^+ \longrightarrow GOx(FADH_2), \quad (7)$$

$$GOx(FADH_2) + O_2 \longrightarrow GOx(FAD) + H_2O_2. \quad (8)$$

When glucose was added into air-saturated PBS, the electrocatalytic reaction was restrained to the enzyme-catalyzed reaction between the oxidized form of GOx, GOx (FAD), and glucose (Eq. 9):

$$\text{Glucose} + \text{GOx(FAD)} \longrightarrow \text{Gluconolactone} + \text{GOx(FADH}_2\text{)}. \quad (9)$$

Thus, according to Eq. (9), with the increase of the concentration of glucose, the reduction peak currents at the GOx/NH_2–Fe@Au/Au electrode gradually decreased as shown in Fig. 6. This study was carried out by SWV. Figure 6 shows the relationship between the decrease of the reduction peak current and the glucose concentration at the GOx/NH_2–Fe@Au/Au electrode. The current values linearly change with the concentration of 2.4–54 mM with a correlation coefficient (R) of 0.9905 and with detection limit of 0.5 mM at $S/N = 3$. The analytical characteristics of glucose determination using different biosensors are compared in table.

Based on the decrease of the reduction current, glucose can be detected without the interference of co-existing electroactive substances, which is different from the common glucose amperometric sensors based on the detection of the consumption of oxygen or the production of hydrogen peroxide [28].

Reproducibility and stability of the GOx/NH_2–Fe@Au modified electrode. The reproducibility of the biosensor response toward glucose was investigated using by the same electrode but carried out on different days. It showed acceptable reproducibilities with RSD of 4.9, 3.7 and 4.6% for five assays of glucose at concentrations of 2, 20 and 40 mM, respectively.

After a storage period of more than two weeks in refrigerator, the biosensor showed no observable change in the cyclic voltammograms. This indicates that not only the covalent binding between NH_2–Fe@Au and oxidized GOx brings about a satisfactory stability but also the magnetic nanocomposite could provide a biocompatible microenvironment for GOx.

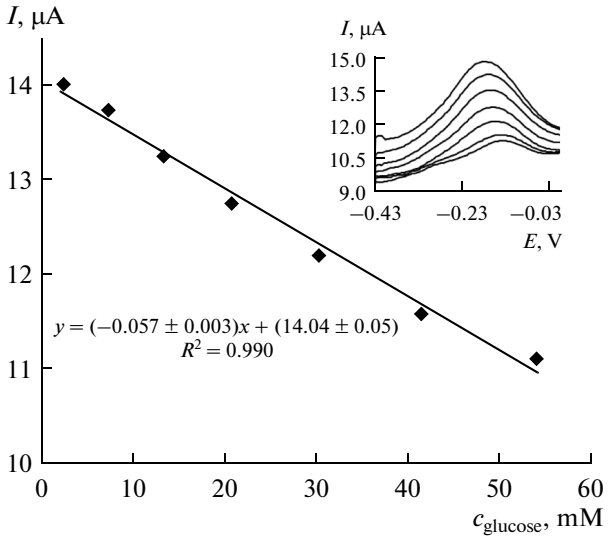

Fig. 6. Calibration curve for the GOx/Fe@Au/Au electrode by SWVs in 0.1 M PBS (pH 6.8) containing various concentrations of glucose (2.4, 7.4 13.4 20.9, 30.4, 42 and 54 mM) at the air-saturated conditions. Inset shows the SWVs of glucose biosensor at scan rate 50 mV/s.

Determination of glucose in serum sample. This glucose biosensor could be applied to assay the real blood glucose. Fresh serum samples were prepared by the affiliated hospital. The serum sample of blood was diluted with phosphate buffer (pH 6.8) to 5 mL. The glucose concentration was determined to be 7.5 ± 0.4 mM ($n = 3$), close to the value of 8.6 ± 0.2 mM ($n = 3$) obtained by spectrophotometry [29].

* * *

We propose a new strategy to prepare a fast, easy and renewable biosensor by immobilizing gold-coated magnetic nanoparticles. GOx was attached to the surface of nanoparticles by cysteamine. The GOx immobilized on the modified electrode exhibits a direct and quasi-reversible electrochemical reaction. The responsibility

Comparison of the analytical parameters obtained in the present work with those reported in the literature

Electrode substrate	Linear range, mM	Detection limit, μM	Sensitivity, μA/mM	Reference
GOx/AuNPs/CPE*	0.04–0.28	10	8.4	[24]
Electrodeposited GOx/AuNPs/Chitosan/Au	0.005–2.4	2.4	Not reported	[25]
Nafion/GOx/f-G-AuNPs**/GCE	Up to 30	1	Not reported	[26]
Graphene/AuNPs/GOx/Chitosan/Au	2–10	180	99.5	[27]
GOx/NH_2–Fe@Au/Au	2.4–54	510	0.057	This work

*—CPE—carbon paste electrode, **—f-G-AuNPs—functionalized graphene sheets with nanocrystalline Au particles.

and linear range is in the scale of glucose in human blood. The constructed biosensor shows a good reproducibility and stability. The procedure is very fast, easy, economical and does not require electrode polishing. It can be use as a glucometer for diabetes patients.

REFERENCES

1. Liu, S. and Ju, H., *Biosens. Bioelectron.*, 2003, vol. 19, p. 177.
2. Wang, K., Xu, J., and Chen, H., *Biosens. Bioelectron.*, 2005, vol. 20, p. 1388.
3. Zhang, S., Wang, N., Yu, H., Niu, Y., and Sun, C., *Bioelectrochemistry*, 2005, vol. 67, p. 15.
4. Zhao, S., Zhang, K., Bai, Y., Yang, W., and Sun, C., *Bioelectrochemistry*, 2006, vol. 69, p. 158.
5. Wang, J., Wang, L., Di, J., and Tu, Y., *Sens. Actuators, B*, 2008, vol. 135, p. 28.
6. Sanchez-Obrero, G., Cano, M., Avila, J.L., Mayen, M., Mena, M.L., Pingarron, J.M., and Rodriguez-Amaro, R., *J. Electroanal. Chem.*, 2009, vol. 634, p. 59.
7. Zhang, S., Wang, N., Niu, Y., and Sun, C., *Sens. Actuators, B*, 2005, vol. 109, p. 367.
8. Qu, S., Wang, J., Kong, J., Yang, P., and Chen, G., *Talanta*, 2007, vol. 71, p. 1096.
9. Huang, H., Liu, X., Zhang, X., Liu, W., Su, X., and Zhang, Z., *Electroanalysis*, 2010, vol. 22, p. 433.
10. Chen, D. and Liao, M., *J. Mol. Catal. B: Enzym.*, 2002, vol. 16, p. 283.
11. Jeong, J., Ha, T.H., and Chung, B.H., *Anal. Chim. Acta.*, 2006, vol. 569, p. 203.
12. Zarei, H., Ghourchian, H., Eskandari, K., and Zeinali, M., *Anal. Biochem.*, 2012, vol. 421, p. 446.
13. Walt, H., Chown, L., Harris, R., Sosibo, N., and Tshikhudo, R., *World Acad. Sci. Eng. Technol.*, 2010, vol. 68, p. 1038.
14. Pham, T.T.H. and Cao, C., *J. Magn. Magn. Mater.*, 2008, vol. 320, p. 2049.
15. Gerber, M., Bodmann, O., and Schulz, G.V., *FEBS Lett.*, 1977, vol. 80, p. 294.
16. Daia, Z., Shao, G., Hong, J., Bao, J., and Shen, J., *Biosens. Bioelectron.*, 2009, vol. 24, p. 1286.
17. Rahimi, P., Rafiee-Pour, H.A., Ghourchian, H., Norouzi, P., and Ganjali, M.R., *Biosens. Bioelectron.*, 2010, vol. 25, p. 130.
18. Shourian, M. and Ghourchian, H., *Sens. Actuators, B*, 2010, vol. 145, p. 607.
19. Deng, C., Chen, J., Chen, X., Xiao, C., Nie, L., and Yao, S., *Biosens. Bioelectron.*, 2008, vol. 23, p. 1272.
20. Cai, C. and Chen, J., *Anal. Biochem.*, 2004, vol. 332, p. 75.
21. Liu, Q., Lu, X., Li, J., Yao, X., and Li, J., *Biosens. Bioelectron.*, 2007, vol. 22, p. 3203.
22. Weibel, M.K. and Bright, H.J., *Biol. Chem.*, 1971, vol. 246, p. 2734.
23. Liu, S. and Ju, H.X., *Biosens. Bioelectron.*, 2003, vol. 19, p. 177.
24. Wang, X., Gu, H., Yin, F., and Tu, Y., *Biosens. Bioelectron.*, 2009, vol. 24, p. 1527.
25. Luo, X., Xu, J., Du, X., and Chen, H., *Anal. Biochem.*, 2004, vol. 334, p. 284.
26. Baby, T.T., Aravind, S.S., Arockiadoss, T., Rakhi, R.B., and Ramaprabhu, S., *Sens. Actuators, B*, 2010, vol. 145, p. 71.
27. Shan, C., Yang, H., Han, D., Zhang, Q., Ivaska, A., and Niu, L., *Biosens. Bioelectron.*, 2010, vol. 25, p. 1070.
28. Deng, C., Chen, J., Chen, X., Xiao, C., Nie, L., and Yao, S., *Biosens. Bioelectron.*, 2008, vol. 23, p. 1272.
29. Liu, S. and Ju, H., *Biosens. Bioelectron.*, 2003, vol. 19, p. 177.